ACS Sustainable Resource Management

pubs.acs.org/acssrm

Article

Upcycling Orange Waste into Bio-Based Aerogels

Laís T. Possari, Patrícia F. Ávila, Michel Brienzo, Caio G. Otoni, Tatiana Budtova,* and Sílvia H. P. Bettini*

Cite This: *ACS Sustainable Resour. Manage.* 2025, 2, 944−952

Read Online

ACCESS | Metrics & More | Article Recommendations | Supporting Information

ABSTRACT: The orange juice industry produces large amounts of by-products. This work introduces new materials based on orange juice side streams—lightweight and high-surface-area aerogels. Orange waste and its fractions (peels, bagasse, and pulp) were first subjected to citric acid hydrolysis, a "green" water-based pre-treatment. Processing parameters (washing with water, biomass fraction, and biomass and citric acid concentrations) were tuned to maximize suspensions' kinetic stability and produce homogenous aerogels. Soluble sugars removal during biomass washing, along with increased biomass and citric acid concentrations led to higher stability of the suspensions, bearing a pectin-rich liquid phase with a dispersed swollen insoluble fraction. Suspensions' rheological properties, insoluble contents, and insoluble fractions' swelling capacities were evaluated. The prepared suspensions were subjected to non-solvent-induced phase separation and solvent exchange with ethanol, followed by drying with supercritical carbon dioxide. Obtained aerogels possessed low densities (<0.1 g/cm^3) and high specific surface areas (190−235 m^2/g). The insoluble swollen fibers were partially porous and embedded in an open-pore nanostructured network.

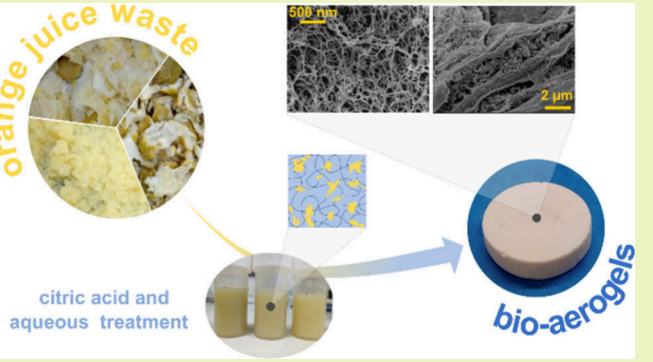

KEYWORDS: *agro-industrial waste, suspension, bioaerogel, porous materials, biopolymers*

1. INTRODUCTION

The production of orange (*Citrus sinensis*) was ca. 70 Mt in 2023.[1] A considerable share (25−30%) of its production is routed to the juice industry,[2,3] where 50 to 60% of the fruits are converted into by-products.[4] When not landfilled, the orange waste is destined mainly for low added-value endings, such as incineration and cattle feeding.[4,5] Upcycling food losses and waste in their integrity (or "bulk" waste)—i.e., without extracting individual components—into bio-based materials has emerged as a promising strategy within the Green Manufacturing and Engineering approach to reduce the use of harsh chemicals, waste generation, and save processing operations, time and energy.[6−8]

To date, materials from bulk orange waste are mainly limited to solvent-cast films using orange peels,[8−14] which are rich in pectin (25−30%, dry basis).[8,15] Acid hydrolysis is frequently used to disrupt the plant tissues and promote pectin extraction into the liquid phase, which then constitutes most of the film's continuous phase, where insoluble fractions are dispersed.[10] Hydrolysis using citric acid has been explored by different authors,[10−14] and films were produced with additives, such as (nano)fillers, cross-linkers,[10,12,13] and/or plasticizers, often glycerol.[8,9,12,16]

Another way to valorize orange waste is to make porous 3D materials, which can find numerous potential applications in packaging, acoustic and thermal insulation, agriculture, etc. Aerogels constitute a special type of porous materials. They are open-pore nanostructured solids, with remarkably low densities (<0.2 g/cm^3) and high specific surface areas (>100 m^2/g). Classical (inorganic and synthetic polymer) aerogels are produced from gels, from which the solvent is removed in such a way that preserve the internal morphology. Bio-based aerogels (also called bio-aerogels) have been systematically invetigated in the past two decades. Most of them are made from neat polysaccharides (e.g., starch, pectin, alginate, chitosan, cellulose, and its derivatives) and, sometimes, proteins.[17−19] Pectin aerogels, for instance, are thermal super-insulating materials[20] and promising drug delivery systems with tuned release kinetics.[21,22] For neat biopolymer aerogels, two main starting matters are known: either solutions with spatially homogeneously distributed polymer chains or suspensions of nanoparticles (e.g., nanocellulose, nanochitin),[23] the latter not being in the scope of this work. Agri-food residual biomasses usually yield heterogeneous systems,

Received: December 12, 2024
Revised: April 25, 2025
Accepted: May 16, 2025
Published: June 13, 2025

comprising a liquid continuous phase and an insoluble fraction as a dispersed phase, encompassing an additional challenge in materials' fabrication: macroscopic phase separation due to the sedimentation. Articles on bio-aerogels made from suspensions (i.e., dissolved polymer + insoluble fraction) are scarce, with few examples known for all-cellulose composite aerogels.[24] The influence of the insoluble fraction on bio-aerogel properties, particularly on pectin-based aerogels, remains unexploited.

Few studies reported on the production of porous materials based on orange waste[25−27] and other citric wastes[28−32] via freeze-drying, resulting in materials with large macropores, which do not correspond to the nanostructured morphology of aerogels. High-specific-surface-area aerogels (>100 m^2/g) from agri-food waste have been reported for other types of agri-food wastes (stale bread,[33] apple pomace, and spent coffee grounds[34]).

This work explores the possibility of using bulk orange waste to produce bio-based aerogels. Wastes from different parts of orange fruits, all after industrial juice extraction, were used and dispersed in water. First, the kinetic stability and other physicochemical properties of orange waste biomass suspensions were evaluated as a function of biomass washing protocol, and biomass and citric acid concentrations. Aerogels were prepared from each biomass fraction and their morphology, density, and specific surface area were discussed and correlated with the suspension properties.

2. EXPERIMENTAL SECTION

2.1. Materials. Orange (*Citrus sinensis*) waste biomass from juice production was donated by JBT Company (Araraquara, Brazil). The orange waste biomass was received in three fractions, namely, peels (flavedo and albedo), bagasse (core, segment walls, and small amounts of seeds and peels), and residual pulp (juice sac membranes) (Figure 1). As informed by the provider, the bulk orange waste

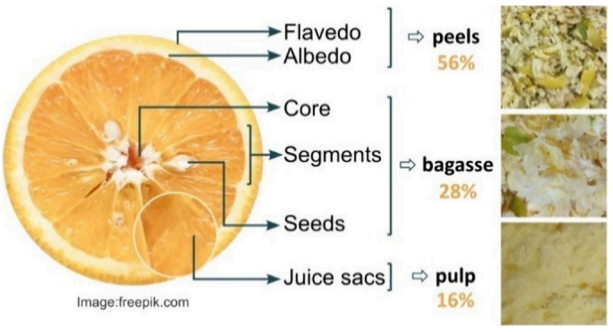

Figure 1. Orange fruit anatomy indicating the parts that originated each biomass fraction. Weight percentages of each fraction in the bulk waste are shown in orange letters.

biomass comprised 56% peels, 28% bagasse, and 16% pulp. A mixture of such fractions at their respective percentages was also used, and referred to as "mixed".

Commercial low-methoxyl (LM) pectin (GENU pectin type LM-102 AS) was donated by CP Kelco (Limeira, Brazil) and used as received. The degree of esterification was 30%, as determined by the manufacturer. Absolute ethanol (99%; Fisher), anhydrous citric acid (Synth), and distilled water were used unless otherwise specified.

2.2. Orange Waste Washing. Each biomass fraction was soaked overnight and rinsed with tap water to remove impurities and soluble sugars (monosaccharides and disaccharides).[11] This procedure was repeated, and the biomass fractions were dried (48 h, at 45 °C, in an air-circulating oven), followed by grinding in liquid nitrogen and sieving (mesh 35, 500 μm). The biomass fractions were finally dried at 45 °C under vacuum for 5 h to remove condensed water and named "washed". The same grinding, drying, and sieving procedures were applied to neither soaked nor rinsed biomass, named "unwashed".

The water-soluble content in both washed and not washed waste mixed biomass was determined by room temperature water extraction (details in the Supporting Information). Water-soluble content was calculated with eq 1

$$\text{water-soluble content (\%)} = 1 - \frac{m_{RT}}{m_i \times (1 - RM)} \times 100 \quad (1)$$

where m_{RT} is the mass of the dried solids collected after extraction and m_i is the initial orange waste mass, which was corrected by the corresponding residual moisture (RM), determined using a Marte ID-50 moisture analyzer at 105 °C (10.7−8.4%).

2.3. Orange Waste Biomass Characterization. The contents of extractives, pectin, and ashes were determined as detailed in the Supporting Information. Ash content was determined by thermogravimetry (TG). The content of extractives was estimated as follows (eq 2)

$$\text{extractives (\%)} = \frac{m_e - m_{fil}}{m_i \times (1 - RM)} \times 100 \quad (2)$$

where m_e is the mass of the filter with the extracted sample after drying and m_{fil} the dried filter mass.

Pectin content in each biomass fraction was calculated with eq 3

$$\text{pectin (\%)} = \frac{m_p - m_{dish}}{m_i \times (1 - RM)} \times 100 \quad (3)$$

where m_p is the mass of the Petri dish with the extracted pectin after drying and m_{dish} is the mass of the Petri dish.

Extractive- and pectin-free samples were used to determine the content of cellulose, hemicellulose and lignin of each fraction using the NREL/TP-510-42618 procedure.[35]

2.4. Suspension Preparation. Each fraction of the biomass (washed or not) was added to citric acid aqueous solutions (concentration of biomass varied from 1 to 4 wt % and of citric acid from 0 to 5 wt %) and hydrolyzed at 90 °C, under vigorous stirring, for 2 h (Figure S1). Suspensions containing individual biomass fractions were labeled "peels", "bagasse", and "pulp". Suspensions were also prepared by mixing the three different fractions in their respective percentages in the bulk biomass (Figure 1) in citric acid solutions; these samples were referred to as "mixed". These suspensions were then used in all subsequent experiments.

2.5. Suspension Characterization. *2.5.1. Rheological Behavior.* Steady-state rheological analyses were conducted with the Couette geometry (2 mm gap) using a TA Instruments ARES rheometer at 23 °C. Shear rate sweeps ranged from 0.1 to 500 s^{-1}.

2.5.2. Kinetic Stability. The suspensions comprised an aqueous phase and an insoluble fraction containing fibers and particles that sedimented with time. In order to make homogeneous aerogels, macroscopic phase separation should be avoided. To find the settings in which sedimentation was minimized, bench physical stability tests were performed on 35 mL of the suspensions produced under different conditions (washed and unwashed biomass, different biomass, and citric acid concentrations) for 3 d at 23 °C. Three days was selected as the average duration of solvent exchange needed to prepare aerogels.

Kinetic stability was calculated using eq 4

$$\text{kinetic stability (\%)} = \frac{V_s}{V_i} \times 100 \quad (4)$$

where V_s is the volume of the sedimented insoluble fraction and V_i is the total volume (35 mL). Graduated tubes were used to measure the volumes.

2.5.3. Insoluble Content, Swelling Capacity, and Morphology. Insoluble content was determined as reported in ref 36: the samples were centrifuged to separate the insoluble fraction from the liquid phase (7698 *g*, 10−15 min), followed by washing with citric acid

https://doi.org/10.1021/acssusresmgt.4c00511
ACS Sustainable Resour. Manage. 2025, 2, 944−952

solutions twice (at the same concentrations as used for suspension preparation) and, then, with water until the supernatant reached pH 6. The samples were centrifuged at 7698 *g* between washings for 10−15 min. The insoluble fraction was dried under vacuum at 105 °C, for 15 h, and weighed (m_{ins}). The insoluble content was calculated by eq 5.

$$\text{insoluble content (\%)} = \frac{m_{ins}}{m_i \times (1 - \text{RM})} \times 100 \quad (5)$$

The water holding capacity (WHC) of the insoluble fractions was calculated using eq 6[37] by measuring the mass of the hydrated (m_h) and dried (m_d) insoluble fractions: m_h was obtained by separating the insoluble fraction from suspensions by centrifuging at 7698 *g* for 15 min, draining excess liquid by inclining the centrifuge tubes at ca. 60 °C for 10 min, and weighing; m_d was obtained by drying the insoluble fractions at 50 °C under vacuum until constant weight.

$$\text{WHC (g/g)} = \frac{m_h - m_d}{m_d} \quad (6)$$

The morphology of insoluble fractions was assessed by optical microscopy using a Keyence VHX 7000 digital microscope (100× and 150× magnifications). The insoluble fractions were washed and dispersed in 45 mL of water. Dispersions were then diluted with water (dilution factor = 5) and sandwiched between glass slides before observation.

2.5.4. Attenuated Total Reflectance−Fourier-Transform Infrared Spectroscopy (ATR-FTIR). The liquid and insoluble fractions of the suspensions were separated by centrifugation (7698 *g*, 15 min), and the polysaccharides present in the liquid phase were precipitated with ethanol. After drying, these polysaccharides and the insoluble fraction were analyzed by FTIR-ATR. Spectra were collected in the range of 4000 to 525 cm^{-1}, with 50 scans and with a 2 cm^{-1} resolution, using a Thermo Nicolet Avatar 370 spectrometer.

2.5.5. Fourier-Transform Raman Spectroscopy (FT-Raman). The polysaccharides precipitated from the liquid phase and insoluble fractions (see previous section) were also analyzed by FT-Raman. Spectra were collected on a Bruker MultiRAM spectrometer with a Nd:YAG laser (1064 nm) (1024 scans, from 3500 to 33 cm^{-1}, 4 cm^{-1} resolution).

2.6. Aerogel Preparation. Each biomass fraction (peels, bagasse, and pulp) and mixed biomass, all hydrolyzed and dispersed in citric acid solutions (see Section 2.4), were used to produce aerogels. Only the conditions (washed/unwashed, biomass, and citric acid concentrations) that provided the best physical stability of suspensions (see Results and Discussion) were selected for aerogels' preparation (Figure S2). Suspensions were poured into polypropylene vials and subjected to mild centrifugation (24 *g*, 1−4 min) to remove air bubbles. To perform drying with supercritical carbon dioxide (CO_2), water in the suspensions was replaced with a liquid miscible with both (in this case, ethanol) through a gradual solvent exchange by pouring a 50/50 ethanol/water mixture on the top of the suspension, triggering a non-solvent-induced phase separation (Figure S2). Gradual increases in ethanol concentration to 75% and 100% were performed in the subsequent exchange steps, followed by several washing steps in pure ethanol until the water concentration in the system was reduced to 0.05%. Stepwise solvent exchange was performed to avoid heterogenous shrinkage.[38] The solvent/non-solvent exchange results in polymers' non-solvent induced phase separation (or immersion precipitation, or coagulation), a well known processing step for making neat bio-based aerogels[18−20] or membranes.[39]

The obtained alcogels were dried with supercritical CO_2 (Figure S2) at the Center for Processes, Renewable Energy and Energy Systems (PERSEE), Mines Paris−PSL. Samples were placed inside a 1 L autoclave, covered with ethanol, and the pressure vessel was closed. CO_2 was introduced, and the pressure increased to approximately 40 bar. As the pressure increased, excess ethanol was purged. Then temperature and pressure were increased to 37 °C and 80 bar, above CO_2 supercritical conditions. A dynamic washing was then performed for 4 h at a flow rate of 50 g of CO_2/min. The system was then depressurized at 4 bar/h, cooled down and samples collected.

The same nomenclature used for the suspensions was used to label aerogels: mixed, peels, bagasse, and pulp. Reference neat LM pectin aerogels were prepared following the same acid pre-treatment and processing steps. All samples were disks with a diameter around 21−22 mm and height around 5−7 mm.

2.7. Aerogel Characterization. *2.7.1. Volumetric Shrinkage.* The volumetric shrinkage induced by solvent exchange and drying was calculated with eq 7

$$\text{shrinkage (\%)} = \frac{V_i - V_f}{V_i} \times 100 \quad (7)$$

where V_i and V_f correspond to the sample volume before and after each processing step, i.e., from suspension to alcogel (solvent exchange) and from alcogel to aerogel (supercritical drying).

2.7.2. Apparent Density and Porosity. To determine the apparent (or bulk) density (ρ_{ap}), the mass of aerogels was measured with a high-precision balance, and the volume was calculated from their height and diameter, taken with a digital caliper with a precision of 0.001 mm.

Porosity was calculated according to eq 8

$$\text{porosity (\%)} = \left(1 - \frac{\rho_{ap}}{\rho_{sk}}\right) \times 100 \quad (8)$$

where ρ_{sk} is the skeletal density, measured by helium pycnometry on an Anton Paar Ultrapyc 5000 Micro device.

2.7.3. Specific Surface Area. The specific surface area was assessed from nitrogen adsorption isotherms performed on a Micromeritics ASAP 2020 using the Brunauer−Emmett−Teller (BET) approach. Samples were degassed under vacuum for 5 h at 70 °C before analyses.

2.7.4. Morphology. A scanning electron microscope (SEM) MAIA 3 (Tescan) was employed to evaluate the aerogels' internal morphology. Before the observations, cryofractured samples were metalized with a 14 nm layer of sputtered platinum using a Q150T Quarum device. 3 kV of accelerating voltage was used.

2.7.5. Intrinsic Viscosity. The influence of the acid pre-treatment on the neat LM pectin molecular weight was calculated from the intrinsic viscosity [η] using a capillary Ubbelhode viscometer (type I, with a 0.63 mm diameter capillary) and an iVisc system from LAUDA. Pectin was solubilized at 60 °C in 0.01 M NaCl and analyzed at 26.6 °C.[40] The average molecular weight (M_v) was estimated as follows

$$[\eta] = K \times M_v^a \quad (9)$$

where K = 0.0234 and a = 0.8221.[40]

3. RESULTS AND DISCUSSION

3.1. Suspension Properties. A preliminary visual screening of 2.5% biomass suspensions (mixed, peels, bagasse, and pulp) in 3% citric acid[10,11,14,41] showed insoluble fraction sedimentation. The production of homogeneous aerogels was, therefore, unfeasible. To find the conditions leading to non-separated suspensions for at least 3−4 days (time needed to complete solvent exchange, Figure S2), the stability and properties of mixed biomass suspensions (see Section 2.4) were first investigated by varying washing/non-washing and biomass and citric acid concentrations. After the optimal conditions in terms of the stability of the mixed biomass suspension were found, the stability of each biomass fraction suspension made with the selected conditions was also investigated.

3.1.1. Influence of Biomass Washing and Concentration on Suspension Properties. First, citric acid concentration was kept at 3%, and the stability of the mixed biomass suspension

https://doi.org/10.1021/acssusresmgt.4c00511
ACS Sustainable Resour. Manage. 2025, 2, 944−952

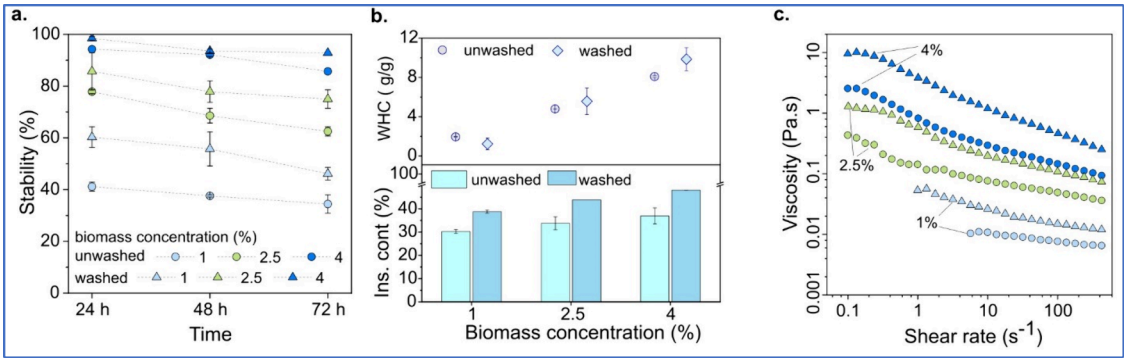

Figure 2. (a) Stability of mixed biomass suspensions over time, (b) water-holding capacity (WHC) and insoluble content as a function of biomass concentration for washed and unwashed samples, and (c) viscosity *vs* shear rate of suspensions of mixed washed (triangles) and unwashed (circles) biomass at different concentrations. The acid concentration was 3%.

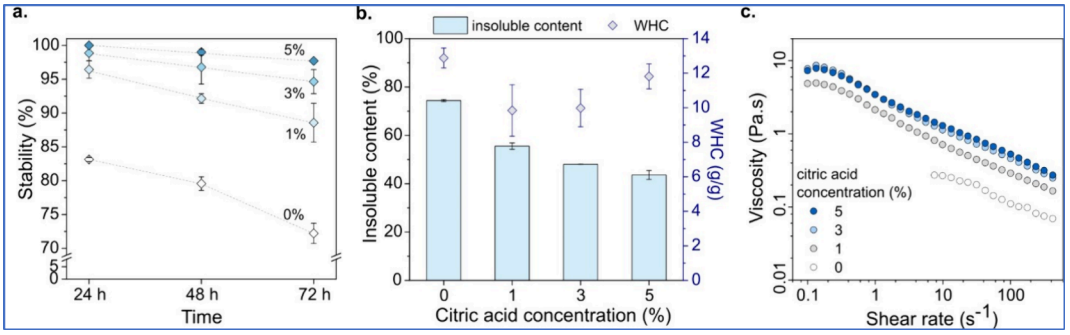

Figure 3. (a) Suspension stability over time, (b) WHC and insoluble content, and (c) viscosity *vs* shear rate for the suspensions of 4% washed mixed biomass at different citric acid concentrations.

was studied as a function of the biomass concentration and the washing/nonwashing step before drying and grinding. As shown in Figure 2a, suspension stability (eq 4) was favored by increasing biomass concentration and the washing step. For example, the stability of samples containing 4% of washed mixed biomass was within 93−98% for 3 days *vs* only 40% for 1% unwashed suspensions. Photos of the suspensions after 72 h are presented in Figure S3a.

The insoluble content (eq 5) increased with biomass concentration, and it was lower for unwashed biomass suspensions (30−37%) when compared with their washed counterparts (39−48%) (Figure 2b). Washing removed low-molecular-weight substances like soluble sugars, organic acids, and certain flavonoids:[42,43] the room temperature water-soluble content decreased from 47.4 ± 0.3% for unwashed to 17 ± 1% for washed samples (eq 1).

The insoluble fraction swelling capacity, expressed as WHC (eq 6), increased with the biomass concentration (Figure 2b). Higher biomass concentration increased inter-particle collisions, which in turn induced inter-particle friction and, potentially, breakage. As a result, the surface area of particles increased, favoring accessibility to water, followed by swelling and increased WHC. WHC was not affected by the washing step (Figure 2b).

The flow curves of washed and unwashed mixed suspensions at different biomass concentrations are presented in Figure 2c. Higher biomass concentrations led to higher viscosities (Figure 2b) due to increased inter-particle friction. Higher viscosities were also observed for washed biomass suspensions compared to their unwashed counterparts due to removal of water-soluble low-molecular-weight compounds during washing, thus increasing the concentration of high-viscosity biopolymers in the liquid phase. Higher viscosities slowed sedimentation and enhanced suspension stability.

Previous studies[44,45] reported that swollen plant fibers can form three-dimensional networks by interacting among themselves and immobilizing the aqueous phase inside said networks, contributing not only to the different rheological behaviors but also to the entrapment of liquid phase, hence limiting phase separation. A more pronounced shear thinning behavior at higher concentrations (Figure 2c) might also reflect the presence of such networks and their disruption under shear stresses.

3.1.2. Influence of Citric Acid Concentration on Suspension Properties. Samples containing 4% washed mixed biomass boasted the best kinetic stability among those analyzed above. However, some phase separation was still observed within the first day (98%), and suspension stability decreased to 93% after 3 days (Figure 2a and Figure S3b). It was previously demonstrated that increasing acid concentration enhanced pectin extraction to the aqueous phase.[46] Therefore, the influence of citric acid concentration on suspension stability, WHC, and the insoluble content was investigated. Mixed biomass concentration was kept at 4%.

The increased acidity improved the stability of the washed mixed biomass suspensions (Figure 3a). This was attributed to the enhanced extraction of pectin into the liquid phase. Although the insoluble content decreased from 74% in the absence of citric acid to about 45% at 5% acid (Figure 3b), the viscosity was increased with higher acid concentration (Figure 3c), corroborating the higher pectin content in the continuous phase. Literature reported that pectin may play an important

https://doi.org/10.1021/acssusresmgt.4c00511
ACS Sustainable Resour. Manage. 2025, 2, 944−952

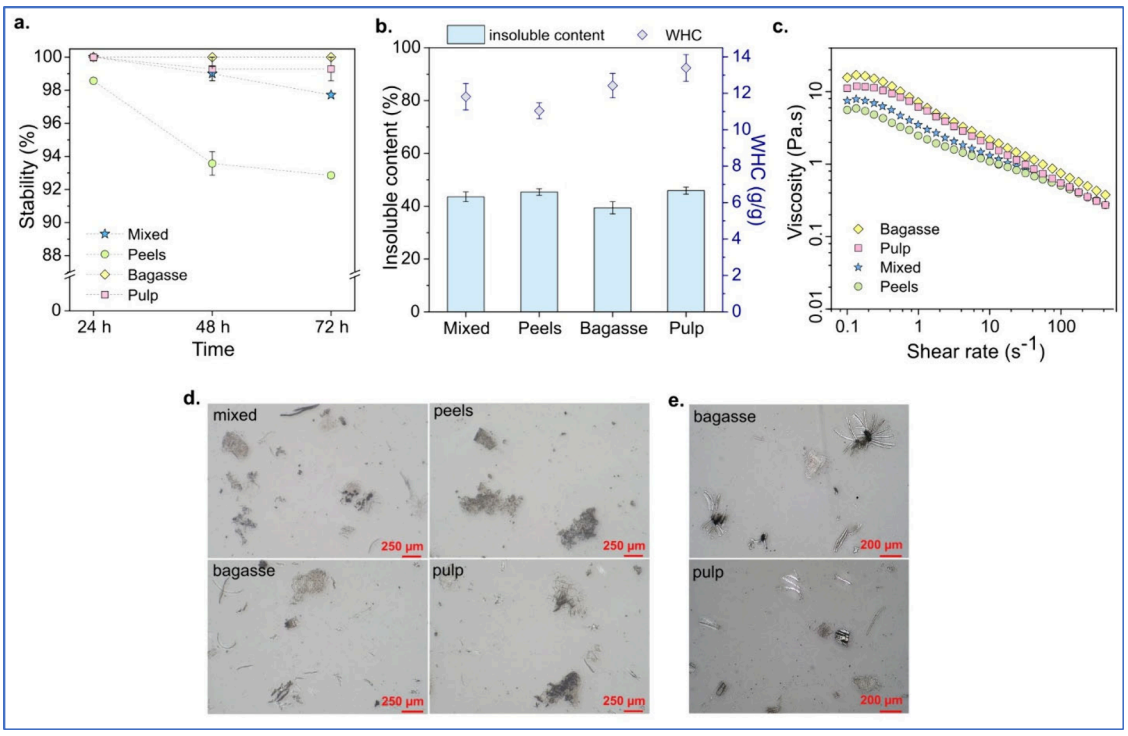

Figure 4. (a) Stability over time, (b) WHC and insoluble content, and (c) viscosity *vs* shear rate for the suspensions containing different biomass fractions. (d) Optical micrographs of the insoluble fractions and (e) zoom-in on bagasse and pulp fibrillated fibers. Parts a, b, and c are for biomass and acid concentrations of 4% and 5%, respectively, and parts d and e are for the same suspensions but diluted (see the Experimental Section).

Table 1. Composition of the Washed Orange Biomass Fractions

	Biomass (%)			
Components	**Mixed**	**Peels**	**Bagasse**	**Pulp**
Ethanol extractives	7.1 ± 0.8	7 ± 1	8.4 ± 0.2	5.7 ± 0.4
Water extractives	30.7 ± 0.9	29 ± 1	34 ± 1	30.8 ± 0.8
Pectin	36 ± 1	35 ± 3	40.5 ± 0.6	32 ± 2
Cellulose	12.8 ± 0.4	14.9 ± 0.7	8.5 ± 0.1	13.2 ± 0.4
Hemicellulose	4.2 ± 0.2	4.8 ± 0.3	3.0 ± 0.3	4.3 ± 0.1
Lignin	5.3 ± 0.7	5 ± 1	2.8 ± 0.4	10 ± 1
Ashes	2.9 ± 0.7	3 ± 1	2.1 ± 0.3	3 ± 1
Total	99	99	99	99

role in improving the kinetic stability of biomass suspensions by acting as a "binder" and structuring the network of insoluble swollen fibers.[47] WHC of the insoluble fraction varied from 10 to 13 g/g and did not depend on acid concentration within the experimental errors (Figure 3b).

3.1.3. Influence of the Biomass Fraction on Suspension Properties. As the suspensions of 4% washed mixed biomass at 5% citric acid remained stable during the first 24 h after the preparation and with 98% stability after 72 h (Figure 3a), these conditions were used to analyze the properties of suspensions made from each biomass fraction: peels, bagasse, and pulp. The bagasse- and pulp-based suspensions showed higher stability (99−100% *vs* 93%, after 72 h) (Figures 4a and S3c) and slightly higher WHC than the peel-based suspension (12−13 g/g *vs* 11 g/g) (Figure 4b), with the latter being of the lowest viscosity (Figure 4c). The insoluble content was the same for all biomass suspensions within experimental errors (Figure 4b).

Optical microscopy images (Figure 4d) suggested that all suspensions had swollen particles of varying dimensions. In particular, bagasse showed a high extent of fibrillation, while the pulp-based ones possessed both particles and fibers (Figure 4e). Peels' insoluble fraction was denser and only fragmented into smaller particles (Figure 4d) as peels possessed a higher content of cellulose when compared to pulp and bagasse (Table 1). In addition, bagasse had the highest contents of extractives (eq 2) and pectin (eq 3). Cellulose is more recalcitrant to the pre-treatment used compared to extractives and pectin;[48] and removing middle lamellae biopolymers, like pectin, was previously linked to fibrillated morphologies of flax fibers.[49] The high degree of fibrillation of the bagasse insoluble particles was likely influenced by its composition (Table 1), contributing also to the higher stability and viscosity of bagasse suspensions. Although pulp and peels had similar cellulose, pectin, and extractives contents, the pulp tissue is softer than the peels and more intensely disrupted during juice extraction,[50,51] facilitating fibrillation and pectin extraction to the aqueous phase. This may have contributed to the higher viscosity and WHC of pulp-based suspensions, thus enhancing the stability.

Hemicellulose content was low and nearly the same for all biomass fractions. Lignin content was different for each

https://doi.org/10.1021/acssusresmgt.4c00511
ACS Sustainable Resour. Manage. 2025, 2, 944−952

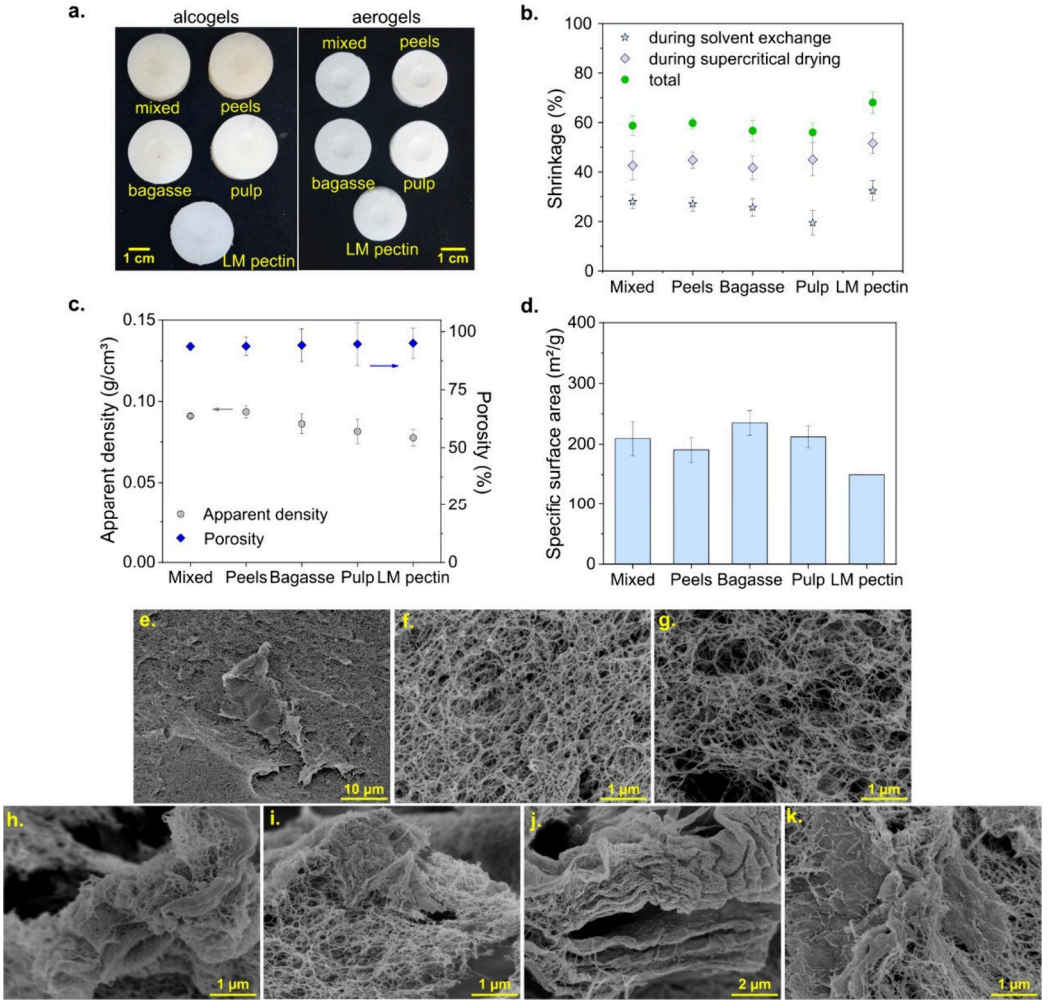

Figure 5. (a) Photos of alcogels and aerogels. (b) Shrinkage of the samples during each step and total shrinkage. (c) Aerogels' porosity and apparent density. (d) Aerogels' specific surface area. Morphology of aerogels based on (e) mixed biomass with insoluble parts embedded in the pectic matrix and (f) the latter at higher magnification, (g) on LM pectin, and of the insoluble fraction of aerogels based on the (h) mixed, (i) peels, (j) bagasse, and (k) pulp fractions.

biomass fraction but lower than pectin, cellulose, and extractives in all cases. FTIR and FT-Raman spectroscopies further evidenced pectin extraction to the liquid phase as a result of the citric acid pre-treatment, while cellulose, hemicellulose, and lignin remained in the insoluble fraction (Supporting Information, Figure S4).

3.2. Aerogel Properties. The conditions leading to the best suspension stability (4% of washed biomass and 5% of citric acid) were used to make aerogels based on mixed biomass, peels, bagasse, and pulp. Commercial LM pectin, pretreated in the same conditions as the biomass, was used as a reference. Non-solvent was added within 3 h after the suspensions' preparation and solvent exchange was completed in 3−4 days (see Section 2.5). The addition of non-solvent decreases the polymer solubility leading to the formation of polymer-rich and polymer-poor phases. Above polymer overlap concentration, a network of polymer-rich phases constitutes the skeleton of the future aerogel. Unlike synthetic polymers, polysaccharides do not entirely collapse during solvent/nonsolvent exchange, creating the tridimensional network of the alcogels. This behavior is attributed to chain rigidity and hydrogen bond polysaccharide−polysaccharide interactions.[39,52]

The alcogels obtained after solvent exchange and the aerogels produced by drying with supercritical CO_2 are shown in Figure 5a. All samples were macroscopically homogeneous and retained the disk-like shape without cracks throughout all preparation steps (Figure 5a).

After solvent exchange and supercritical drying, all samples underwent volumetric shrinkage (Figure 5b) of ca. 55−70%, similar to previously reported values for aerogels from other bio-based sources, such as neat pectin[53] and cellulose.[54] The shrinkage of pulp- and bagasse-based samples was slightly lower than that of the other materials, which might be related to the higher viscosity of the respective suspensions and stronger networks due to greater swelling and fibrillation of the insoluble fractions. These aspects possibly helped samples to resist contraction in the presence of the non-solvent, i.e., ethanol. The highest shrinkage was for neat LM pectin samples.

The apparent density of the aerogels is presented in Figure 5c. It varied from 0.08 to 0.09 g/cm^3 for all samples. Despite the higher volumetric shrinkage of neat LM pectin samples, its aerogel had a density similar to that of other biomass-based aerogels. The presence of non-dissolved particles in the biomass-based aerogels outweighed the lower shrinkage.

https://doi.org/10.1021/acssusresmgt.4c00511
ACS Sustainable Resour. Manage. 2025, 2, 944−952

Aerogels made from the different biomass fractions and mixed orange waste biomass suspensions yielded high porosities and low densities despite having a high insoluble content. The reason was that non-dissolved particles and fibers were swollen (Figure 4) and remained porous after solvent exchange and drying. This was confirmed by the high specific surface area of all obtained aerogels, 190−235 m^2/g (Figure 5d). Usually, non-swollen fibers decrease the specific surface area, as demonstrated for all-cellulose aerogels,[24] which was not the case for orange waste biomass-based aerogels. Similar surface areas were also reported for aerogels derived from neat polysaccharides like starch and cellulose,[17] cellulose aerogel composites with insoluble fibers,[24] and aerogels based on apple pomace and spent coffee grounds.[34]

Orange waste biomass-based aerogels boasted similar properties as those produced from different neat biopolymers for packaging,[56] drug delivery[57] and food[58] applications, hence presenting potential to be further explored. Notably, biomasses with somewhat different compositions, as seen in Table 1, yielded porous materials with similar properties.

Neat LM pectin aerogel showed the lowest surface area, 150 m^2/g—much lower than that of non-treated LM pectin aerogels made from pectin solutions (around 500−600 m^2/g).[53] The acid pre-treatment degraded the polymer, leading to a weaker gel. The molecular weight of pectin in the aerogel was 104 kg/mol *vs* 131 kg/mol for the initial pectin. A decreased surface area due to the lower molecular weight of the polymer was also reported for hyaluronic acid-based aerogels.[55] Therefore, acidic hydrolysis had a decisive impact on aerogel properties: on one hand, it allowed swelling and fibrillation of non-dissolved parts and production of homogeneous samples, but on the other hand, it decreased pectin molecular weight.

SEM observations confirmed the hypotheses mentioned above (Figure 5e−k). The obtained aerogels exhibited a nanostructured open-pore fibrillar network as a continuous phase (Figure 5e−g) with well-dispersed swollen insoluble particles and fibers (Figure 5h−k). The continuous phase morphology was remarkably similar to the LM pectin aerogels' texture (Figure 5g), further supporting the assumption that it was composed mainly of pectin, while cellulose and hemicellulose remained mainly insoluble, as suggested by FTIR and FT-Raman analyses (Figure S4). For the neat LM pectin aerogel, SEM images revealed a partially damaged network (Figure 5g), confirming its low specific surface area.

4. CONCLUSIONS

The upcycling of orange waste biomass, suspended and hydrolyzed, into aerogels was explored by varying biomass preparation (washing or non-washing), and biomass and acid concentrations. To avoid precipitation of solids, suspension stability was first investigated to select the optimal preparation conditions. Suspensions' kinetic stability was greater with washed biomass and higher concentrations of biomass and citric acid. Washing removed low-molecular-weight substances, while higher biomass concentration increased the viscosity and the insoluble fractions' water holding capacity. Higher acidity enhanced pectin extraction and decreased the insoluble content. The influence of the biomass fraction (peels, bagasse, and pulp) on the suspension stability was also evaluated. Pulp and bagasse suspensions had higher stability and viscosity due to fibrillated insoluble fractions and a higher WHC.

Aerogels from orange peels, bagasse, pulp, and their mixture presented low density (0.08−0.09 g/cm^3), high porosity (94−95%), and high specific surface area (190−235 m^2/g). Aerogel morphology comprised a fine network of pectin fibrils as the continuous phase, with embedded non-dissolved porous fibers and particles. No significant influence of the biomass type on aerogel properties was recorded, except for LM pectin.

This work presents a new approach to valorize bulk orange waste biomass into high-added-value bio-based aerogels. The resulting aerogels can be used in numerous applications, such as packaging, adsorption or absorption, and delivery devices of different active substances for food and agriculture.

■ ASSOCIATED CONTENT

Supporting Information

The Supporting Information is available free of charge at https://pubs.acs.org/doi/10.1021/acssusresmgt.4c00511.

Orange waste biomass characterization methodology details, illustrative schemes of suspension and aerogel preparation, photos of suspensions after 72 h, and FTIR and FT-Raman spectra of the insoluble fraction of the suspensions and the polysaccharides precipitated from the liquid phase (PDF)

■ AUTHOR INFORMATION

Corresponding Authors

Tatiana Budtova − *Mines Paris, PSL University, Center for Materials Forming (CEMEF), 06904 Sophia Antipolis, France;* orcid.org/0000-0003-1835-2146; Email: tatiana.budtova@minesparis.psl.eu

Sílvia H. P. Bettini − *Federal University of São Carlos (UFSCar), Graduate Program in Materials Science and Engineering (PPGCEM) and Department of Materials Engineering (DEMa), São Carlos, SP 13565-905, Brazil;* orcid.org/0000-0001-6549-2980; Email: silvia.bettini@ufscar.br

Authors

Laís T. Possari − *Federal University of São Carlos (UFSCar), Graduate Program in Materials Science and Engineering (PPGCEM), São Carlos, SP 13565-905, Brazil; Mines Paris, PSL University, Center for Materials Forming (CEMEF), 06904 Sophia Antipolis, France;* orcid.org/0000-0002-7167-1966

Patrícia F. Ávila − *São Paulo State University (UNESP), Institute for Research in Bioenergy (IPBEN), Rio Claro, SP 13500-230, Brazil*

Michel Brienzo − *São Paulo State University (UNESP), Institute for Research in Bioenergy (IPBEN), Rio Claro, SP 13500-230, Brazil*

Caio G. Otoni − *Federal University of São Carlos (UFSCar), Graduate Program in Materials Science and Engineering (PPGCEM), São Carlos, SP 13565-905, Brazil; University of Campinas (UNICAMP), Institute of Chemistry, Campinas, SP 13083-862, Brazil;* orcid.org/0000-0001-6734-7381

Complete contact information is available at: https://pubs.acs.org/10.1021/acssusresmgt.4c00511

Funding

The Article Processing Charge for the publication of this research was funded by the Coordenacao de Aperfeicoamento de Pessoal de Nivel Superior (CAPES), Brazil (ROR identifier: 00x0ma614).

Notes

The authors declare no competing financial interest.

■ ACKNOWLEDGMENTS

This study was financed in part by the *Coordenação de Aperfeiçoamento de Pessoal de Nível Superior - Brasil* (CAPES) - Finance Code 001. Funding was provided by the CAPES (grant nos. 88887.671778/2022-00 and 88887.836065/2023-00), the São Paulo Research Foundation (grant no. 2021/12071-6), and the Brazilian National Council for Scientific and Technological Development (CNPq) through the INCT Circularity in Polymer Materials (grant no. 406925/2022-4). The authors are grateful to Julien Jaxel (PERSEE, Mines Paris) for the supercritical drying, Frédéric Georgi (CEMEF, Mines Paris) for the guidance with SEM and optical microscopy, Rafaella Ferreira Fernandes (FZEA-USP/DEMa-UFSCar) for the Raman spectroscopy measurements, JBT Company for donating the orange waste, and CP Kelco for providing pectin. C. G. Otoni and S. H. P. Bettini are thankful to CNPq (grants no. 304753/2022-0 and 312570/2023-6). Article processing charges were financed by CAPES through the CAPES-ACS consortium.

■ REFERENCES

(1) FAO. FAOSTAT Analytical Brief 96 - Agricultural Production Statistics 2010−2023; 2024. https://openknowledge.fao.org/server/api/core/bitstreams/df90e6cf-4178-4361-97d4-5154a9213877/content (accessed March 31, 2025).

(2) Sharma, K.; Mahato, N.; Cho, M. H.; Lee, Y. R. Converting Citrus Wastes into Value-Added Products: Economic and Environmently Friendly Approaches. *Nutrition* **2017**, *34*, 29−46.

(3) Panwar, D.; Saini, A.; Panesar, P. S.; Chopra, H. K. Unraveling the Scientific Perspectives of Citrus By-Products Utilization: Progress towards Circular Economy. *Trends Food Sci. Technol.* **2021**, *111*, 549−562.

(4) Teigiserova, D. A.; Tiruta-Barna, L.; Ahmadi, A.; Hamelin, L.; Thomsen, M. A Step Closer to Circular Bioeconomy for Citrus Peel Waste: A Review of Yields and Technologies for Sustainable Management of Essential Oils. *J. Environ. Manage.* **2021**, *280*, No. 111832.

(5) Gaur, A.; Tiwari, S.; Kumar, C.; Maiti, P. Bio-Waste Orange Peel and Polymer Hybrid for Efficient Energy Harvesting. *Energy Reports* **2020**, *6*, 490−496.

(6) Otoni, C. G.; Azeredo, H. M. C.; Mattos, B. D.; Beaumont, M.; Correa, D. S.; Rojas, O. J. The Food−Materials Nexus: Next Generation Bioplastics and Advanced Materials from Agri-Food Residues. *Adv. Mater.* **2021**, *33* (43), No. 2102520.

(7) Vieira, R. M.; de Freitas, C.; Beluomini, M. A.; Silva, R. D.; Stradiotto, N. R.; de Azeredo, H. M. C.; Brienzo, M. Exploring Fruit Waste Macromolecules and Their Derivatives to Produce Building Blocks and Materials. *Rev. Environ. Sci. Bio/Technology* **2025**, *24* (1), 167−189.

(8) Santos, L. B.; Silva, R. D.; Alonso, J. D.; Brienzo, M.; Silva, N. C.; Perotto, G.; Otoni, C. G.; Azeredo, H. M. C. Bioplastics from Orange Processing Byproducts by an Ecoefficient Hydrothermal Approach. *Food Packag. Shelf Life* **2023**, *38*, No. 101114.

(9) Yaradoddi, J. S.; Banapurmath, N. R.; Ganachari, S. V.; Soudagar, M. E. M.; Sajjan, A. M.; Kamat, S.; Mujtaba, M. A.; Shettar, A. S.; Anqi, A. E.; Safaei, M. R.; Elfasakhany, A.; Haque Siddiqui, M. I.; Ali, M. A. Bio-Based Material from Fruit Waste of Orange Peel for Industrial Applications. *J. Mater. Res. Technol.* **2022**, *17*, 3186−3197.

(10) Quilez-Molina, A. I.; Mazzon, G.; Athanassiou, A.; Perotto, G. A Novel Approach to Fabricate Edible and Heat Sealable Bio-Based Films from Vegetable Biomass Rich in Pectin. *Mater. Today Commun.* **2022**, *32* (June), No. 103871.

(11) Bátori, V.; Jabbari, M.; Åkesson, D.; Lennartsson, P. R.; Taherzadeh, M. J.; Zamani, A. Production of Pectin-Cellulose Biofilms: A New Approach for Citrus Waste Recycling. *Int. J. Polym. Sci.* **2017**, *2017*, No. 9732329.

(12) Bátori, V.; Lundin, M.; Åkesson, D.; Lennartsson, P. R.; Taherzadeh, M. J.; Zamani, A. The Effect of Glycerol, Sugar, and Maleic Anhydride on Pectin-Cellulose Thin Films Prepared from Orange Waste. *Polymers (Basel).* **2019**, *11* (3), 392.

(13) Mousavi Kalajahi, S. E.; Alizadeh, A.; Hamishehkar, H.; Almasi, H.; Asefi, N. Orange Juice Processing Waste as a Biopolymer Base for Biodegradable Film Formation Reinforced with Cellulose Nanofiber and Activated with Nettle Essential Oil. *J. Polym. Environ.* **2022**, *30* (1), 258−269.

(14) Merino, D.; Simonutti, R.; Perotto, G.; Athanassiou, A. Direct Transformation of Industrial Vegetable Waste into Bioplastic Composites Intended for Agricultural Mulch Films. *Green Chem.* **2021**, *23* (16), 5956−5971.

(15) Wan Chik, M. A.; Yusof, R.; Shafie, M. H.; Mohamed Hanaphi, R. The Versatility of Pectin: A Comprehensive Review Unveiling Its Recovery Techniques and Applications in Innovative Food Products. *J. Food Meas. Charact.* **2024**, *18* (7), 6101−6123.

(16) Moaveni, R.; Ghane, M.; Soltani, P.; Zamani, A.; Ramamoorthy, S. K. Production of Polymeric Films from Orange and Ginger Waste for Packaging Application and Investigation of Mechanical and Thermal Characteristics of Biofilms. *Applied Sciences.* **2024**, *14*, 4670.

(17) Budtova, T.; Aguilera, D. A.; Beluns, S.; Berglund, L.; Chartier, C.; Espinosa, E.; Gaidukovs, S.; Klimek-kopyra, A.; Kmita, A.; Lachowicz, D.; Liebner, F.; Platnieks, O.; Rodríguez, A.; Navarro, L. K. T.; Zou, F.; Buwalda, S. J. Biorefinery Approach for Aerogels. *Polymers (Basel).* **2020**, *12* (12), 2779.

(18) Yu, S.; Budtova, T. Creating and Exploring Carboxymethyl Cellulose Aerogels as Drug Delivery Devices. *Carbohydr. Polym.* **2024**, *332*, No. 121925.

(19) Viola, M.; Chartier, C.; Mihajlovic, M.; Buwalda, S.; Pradille, C.; Budtova, T.; Vermonden, T. Exploring Silk Fibroin Aerogels via Different Coagulation Approaches. *Eur. Polym. J.* **2024**, *205*, No. 112722.

(20) Groult, S.; Budtova, T. Thermal Conductivity/Structure Correlations in Thermal Super-Insulating Pectin Aerogels. *Carbohydr. Polym.* **2018**, *196* (2018), 73−81.

(21) Groult, S.; Buwalda, S.; Budtova, T. Tuning Bio-Aerogel Properties for Controlling Theophylline Delivery. Part 1: Pectin Aerogels. *Mater. Sci. Eng. C* **2021**, *126*, No. 112148.

(22) De Cicco, F.; Russo, P.; Reverchon, E.; García-González, C. A.; Aquino, R. P.; Del Gaudio, P. Prilling and Supercritical Drying: A Successful Duo to Produce Core-Shell Polysaccharide Aerogel Beads for Wound Healing. *Carbohydr. Polym.* **2016**, *147*, 482−489.

(23) Zou, F.; Budtova, T. Polysaccharide-Based Aerogels for Thermal Insulation and Superinsulation: An Overview. *Carbohydr. Polym.* **2021**, *266*, No. 118130.

(24) Korhonen, O.; Budtova, T. All-Cellulose Composite Aerogels and Cryogels. *Compos. Part A Appl. Sci. Manuf.* **2020**, *137*, No. 106027.

(25) Xiao, S.; Zou, M.; Xie, Y.; Chen, W.; Hu, X.; Ma, Y.; Zu, S.; Che, Y.; Jiang, X. Nanosilver Modified Navel Orange Peel Foam/Polyethylene Glycol Composite Phase Change Materials with Improved Thermal Conductivity and Photo-Thermal Conversion Efficiency. *J. Energy Storage* **2022**, *56*, No. 105976.

(26) Suchorowiec, K.; Bieda, M.; Szatkowska, M.; Sieradzka, M.; Kuźnia, M.; Ziąbka, M.; Pielichowska, K. From Waste to Functional Material—Carbon Aerogels from Citrus Biomass Infiltrated with Phase Change Materials for Possible Application in Solar-Thermal Energy Conversion and Storage. *Energies.* **2025**, *18*, 814.

(27) Gao, F.; Qiu, Z.; Hou, Y.; You, Y.; Lv, X.; Dang, J. Novel Aerogel of Aminated MXene Composite Orange Peel Biomass for Ultra-High Capacity of V(V) Adsorption. *Colloids Surfaces A Physicochem. Eng. Asp.* **2024**, *697*, No. 134472.

(28) Imran, M.; Islam, A.; Ismail, F.; Zhang, P.; Basharat, M.; Ikram, M.; Uddin, A.; Zeb, S.; Hassan, Q.-U.; Gao, Y. 3D Porous Superoleophilic/Hydrophobic Grapefruit Peel Aerogel for Efficient Removal of Emulsified-Oil from Water. *J. Environ. Chem. Eng.* **2023**, *11* (2), No. 109324.
(29) Wang, H.; Wang, P.; Kasapis, S.; Truong, T. Aerogel-Based Oil Sorbents Derived from Pomelo (Citrus Grandis L.) Peels as Potential Gel Matrices for Food Applications: Formation, Properties and in-Vitro Oral Processing. *J. Food Eng.* **2025**, *394*, No. 112532.
(30) Li, L.; Jin, Z.; Wang, C.; Wang, Y.-C. Valorization of Food Waste: Utilizing Natural Porous Materials Derived from Pomelo-Peel Biomass to Develop Triboelectric Nanogenerators for Energy Harvesting and Self-Powered Sensing. *ACS Appl. Mater. Interfaces* **2024**, *16* (29), 37806−37817.
(31) Pung, T.; Jitchum, V.; Srisang, S.; Vichitbandh, P.; Panich-pat, T. Carbonaized Carbon Aerogels Derived from Pomelo Peels for Sorption of Some Organic Solvents. *Agric. Nat. Resour.* **2024**, *58* (1), 81−88.
(32) Liu, Y.; Lei, X.; Cao, J.; Pang, Y.; Wang, L.; Zhang, T. Carbon Aerogel with Solid and Magnetic Coating Prepared from Freeze-Thawed Pomelo Peel Waste for Oil Adsorption. *J. Environ. Chem. Eng.* **2025**, *13* (2), No. 115943.
(33) Guo, W.; Budtova, T.; Martinez, M. M. Upcycling Stale Bread into (Meso)Porous Materials: Xerogels and Aerogels. *Food Hydrocoll.* **2025**, *160*, No. 110807.
(34) Gaggero, G.; Subrahmanyam, R. P.; Schroeter, B.; Gurikov, P.; Delucchi, M. Organic Bio-Based Aerogel from Food Waste: Preparation and Hydrophobization. *Gels.* **2022**, *8*, 691.
(35) Sluiter, J.; Sluiter, A.; Scarlata, C.; Templeton, D.; Crocker, D.; Hames, B. Determination of Structural Carbohydrates and Lignin in Biomass: Laboratory Analytical Procedure (LAP) (Revised August 2012); National Renewable Energy Laboratory (NREL): 2008; p 18. https://www.nrel.gov/docs/gen/fy13/42618.pdf.
(36) Korhonen, O.; Sawada, D.; Budtova, T. All-Cellulose Composites via Short-Fiber Dispersion Approach Using NaOH−Water Solvent. *Cellulose* **2019**, *26* (8), 4881−4893.
(37) Valoppi, F.; Wang, Y.-J.; Alt, G.; Peltonen, L. J.; Mikkonen, K. S. Valorization of Native Soluble and Insoluble Oat Side Streams for Stable Suspensions and Emulsions. *Food Bioprocess Technol.* **2021**, *14*, 751−764.
(38) Gurikov, P.; S. P, R.; Griffin, J. S.; Steiner, S. A. I. I. I.; Smirnova, I. 110th Anniversary: Solvent Exchange in the Processing of Biopolymer Aerogels: Current Status and Open Questions. *Ind. Eng. Chem. Res.* **2019**, *58* (40), 18590−18600.
(39) Budtova, T. Cellulose II Aerogels: A Review. *Cellulose* **2019**, *26* (1), 81−121.
(40) Masuelli, M. A. Mark-Houwink Parameters for Aqueous-Soluble Polymers and Biopolymers at Various Temperatures. *J. Polym. Biopolym. Phys. Chem.* **2014**, *2* (2), 37−43.
(41) Ghasemizad, S.; Pirsa, S.; Amiri, S.; Abdosatari, P. Optimization and Characterization of Bioactive Biocomposite Film Based on Orange Peel Incorporated with Gum Arabic Reinforced by Cr2O3 Nanoparticles. *J. Polym. Environ.* **2022**, *30*, 2493−2506.
(42) Vallejo, F.; Larrosa, M.; Escudero, E.; Zafrilla, M. P.; Cerdá, B.; Boza, J.; García-Conesa, M. T.; Espín, J. C.; Tomás-Barberán, F. A. Concentration and Solubility of Flavanones in Orange Beverages Affect Their Bioavailability in Humans. *J. Agric. Food Chem.* **2010**, *58* (10), 6516−6524.
(43) Sharma, K.; Mahato, N.; Lee, Y. R. Extraction, Characterization and Biological Activity of Citrus Flavonoids. *Reviews in Chemical Engineering* **2019**, *35* (2), 265−284.
(44) Lin, J.; Tang, Z.; Brennan, C. S.; Zeng, X. Thermomechanically Micronized Sugar Beet Pulp: Dissociation Mechanism, Physicochemical Characteristics, and Emulsifying Properties. *Food Res. Int.* **2022**, *160*, No. 111675.
(45) Yin, Z.; Wang, Z.; He, Z.; Zeng, M.; Qin, F.; Chen, J. Effect of Particle Size and Microstructure on the Physical Properties of Soybean Insoluble Dietary Fiber in Aqueous Solution. *Food Biosci.* **2021**, *41*, No. 100898.
(46) Pasandide, B.; Khodaiyan, F.; Mousavi, Z.; Hosseini, S. S. Pectin Extraction from Citron Peel: Optimization by Box−Behnken Response Surface Design. *Food Sci. Biotechnol.* **2018**, *27* (4), 997−1005.
(47) Ptaszek, P.; Basu, S. Influence of Fibers and Particle Size Distribution on Food Rheology. In *Advances in Food Rheology and its Applications*; Ahmed, J., Ed.; Woodhead Publishing: 2016; pp 177−208. DOI: 10.1016/B978-0-08-100431-9.00008-5.
(48) Bajpai, P. Biomass Composition. In *Biomass to Energy Conversion Technologies: The Road to Commercialization*; Elsevier: Amsterdam, The Netherlands, 2020; pp 31−40. DOI: 10.1016/B978-0-12-818400-4.00004-9.
(49) Gautreau, M.; Durand, S.; Paturel, A.; Le Gall, S.; Foucat, L.; Falourd, X.; Novales, B.; Ralet, M.-C.; Chevallier, S.; Kervoelen, A.; Bourmaud, A.; Guillon, F.; Beaugrand, J. Impact of Cell Wall Non-Cellulosic and Cellulosic Polymers on the Mechanical Properties of Flax Fibre Bundles. *Carbohydr. Polym.* **2022**, *291*, No. 119599.
(50) Jentzsch, M.; Albiez, V.; Kardamakis, T. C.; Speck, T. Analysis of the Peel Structure of Different Citrus Spp. via Light Microscopy, SEM and MCT with Manual and Automatic Segmentation. *Soft Matter* **2024**, *20* (12), 2804−2811.
(51) Berk, Z. By-Products of the Citrus Processing Industry. In *Citrus Fruit Processing*; Berk, Z., Ed.; Academic Press: San Diego, CA, 2016; pp 219−233. DOI: 10.1016/B978-0-12-803133-9.00010-2.
(52) Innocenzi, P. Overview of the Sol−Gel Process. In *Springer Handbook of Aerogels*; Aegerter, M. A., Leventis, N., Koebel, M., Steiner, S. A., III, Eds.; Springer International Publishing: Cham, Switzerland, 2023; pp 53−69. DOI: 10.1007/978-3-030-27322-4_2.
(53) Groult, S.; Budtova, T. Tuning Structure and Properties of Pectin Aerogels. *Eur. Polym. J.* **2018**, *108*, 250−261.
(54) Buchtová, N.; Budtova, T. Cellulose Aero- , Cryo- and Xerogels: Towards Understanding of Morphology Control. *Cellulose* **2016**, *23*, 2585−2595.
(55) Aguilera-bulla, D.; Legay, L.; Buwalda, S. J.; Budtova, T. Crosslinker-Free Hyaluronic Acid Aerogels. *Biomacromolecules* **2022**, *23*, 2838−2845.
(56) Manzocco, L.; Mikkonen, K. S.; García-González, C. A. Aerogels as Porous Structures for Food Applications: Smart Ingredients and Novel Packaging Materials. *Food Struct.* **2021**, *28*, No. 100188.
(57) Groult, S.; Buwalda, S.; Budtova, T. Tuning Bio-Aerogel Properties for Controlling Drug Delivery. Part 2: Cellulose-Pectin Composite Aerogels. *Biomater. Adv.* **2022**, *135*, No. 212732.
(58) Ciuffarin, F.; Négrier, M.; Plazzotta, S.; Libralato, M.; Calligaris, S.; Budtova, T.; Manzocco, L. Interactions of Cellulose Cryogels and Aerogels with Water and Oil: Structure-Function Relationships. *Food Hydrocoll.* **2023**, *140*, No. 108631.